

# Hadronic interaction model dependence in cosmic Gamma-ray flux estimation using a surface air shower array with an underground muon detector

---

**S.Okukawa<sup>a,\*</sup> for the ALPACA collaboration**

(a complete list of authors can be found at the end of the proceedings)

<sup>a</sup>*Faculty of Engineering, Yokohama National University, Yokohama 240-8501, Japan*

*E-mail: [okukawa-sousuke-dt@ynu.jp](mailto:okukawa-sousuke-dt@ynu.jp)*

The ALPACA detector is currently being constructed to study high-energy gamma-ray astronomy in the SubPeV region of the southern galactic sky. The ALPACA consists of a ground-based air shower detector array (AS) and an underground muon detector array (MD) installed underground, and this experiment uses the muon intensity measured by MD to increase sensitivity to cosmic gamma rays. This study evaluated the hadronic interaction model dependence in the detection efficiency of gamma-ray-induced air showers using the ALPAQUITA configuration, which is the prototype of the ALPACA. The model dependence on hadronic interactions is smaller than 3.6 % in the typical gamma-ray flux estimation performed by ALPAQUITA. This is negligible compared with other uncertainties such as absolute energy scale uncertainty in the energy range from 6 to 300 TeV, which is dominated by the Monte Carlo statistics. We also expect this small model dependence can be applied to ALPACA.

38th International Cosmic Ray Conference (ICRC2023)  
26 July - 3 August, 2023  
Nagoya, Japan



---

\*Speaker

## 1. Introduction

Astronomical observation using electromagnetic waves has been conducted in a wide energy range, from radio waves to gamma rays. Gamma-ray observations around the PeV region are currently the highest energy region. Such observational research is important to study the origin of cosmic rays in our galaxy and astronomical phenomena within a few Mpc. However, the intensity of such high-energy gamma rays is extremely low. The only practical method is to use a ground-based air shower detector which has a large effective area. Moreover, separating between gamma-ray/cosmic-ray induced air shower ( $\gamma$ -CR separation) to reject the large amounts of hadronic cosmic rays that act as a background is essential for measuring faint gamma rays in these experiments. One method is to leverage the muon-poor nature of gamma-ray-induced air showers to separate them from hadronic cosmic-ray-induced air showers [1]. Tibet AS $\gamma$  deploys a 65,700 m<sup>2</sup> surface-type particle detector array comprising 597 plastic scintillation detectors arranged in a grid pattern on the Tibet plateau at an altitude of 4,300 m to continuously observe hadronic cosmic-ray/gamma-ray-induced air showers above several TeV [2]. A large underground water Cherenkov muon detector is installed 2.4 m below the surface detector array on the ground to separate gamma-ray-induced muon-poor air showers from hadronic-cosmic-ray-induced muon-rich air showers [3, 4]. This method enables to remove 98.9 % and 99.92 % of hadronic cosmic rays at 10 and 100 TeV, respectively. Such techniques require Monte Carlo simulations of air shower development to evaluate the measurement performances. Thus, differences in hadronic interaction models in air shower development can cause systematic uncertainties in the detection efficiency of the gamma-ray-induced air showers using the number of muons as a selection criterion. To avoid this dependence, Tibet AS $\gamma$  experimentally estimates the background hadronic cosmic rays using air showers from directions away from the gamma-ray point source to measure the flux [2]. On the other hand, systematic uncertainties in the detection efficiency of the gamma-ray induced air showers using the number of muons as a selection criterion remain. However, the hadronic interaction model dependence of the gamma-ray-induced air showers is believed to be small and may be ignored, then the model dependence has yet to be quantified. This paper evaluated the systematic differences in the detection efficiency of gamma-ray-induced air showers caused by the  $\gamma$ -CR separation in the energy range from a few TeV to several hundred TeV with a small air shower array (ALPAQUITA [5]), which is the prototype of ALPACA [6, 7].

## 2. Survival ratio of gamma rays

To estimate gamma-ray flux from experimental data, we require to evaluate the survival ratio of gamma rays ( $R_i^{\text{surv}}(E_\gamma)$ ) after the  $\gamma$ -CR separation using the number of measured muons using Monte Carlo simulation. Therefore, we examined the interaction model dependencies.

$R_i^{\text{surv}}(E_\gamma)$  is calculated as

$$R_i^{\text{surv}}(E_\gamma) = \frac{N_{\text{sim}}^{\text{rec}, \gamma\text{-like}}(E_\gamma)}{N_{\text{sim}}^{\text{rec}}(E_\gamma)}, \quad (1)$$

where  $N_{\text{sim}}^{\text{rec}}(E_\gamma)$  is the number of reconstructed gamma-ray events, and  $N_{\text{sim}}^{\text{rec}, \gamma\text{-like}}(E_\gamma)$  denotes the number of events deemed gamma-like among  $N_{\text{sim}}^{\text{rec}}(E_\gamma)$ . The index  $i$  represents hadronic interaction model used for air shower simulation as mentioned in Section 2.1.

## 2.1 Air shower simulation and simulation setting

Assuming a gamma-ray source with a power-law energy spectrum with a spectral index of -2 in the direction of RX J1713.7-394, we generated  $10^8$  gamma-ray air showers in the energy range from 300 GeV to 10 PeV with CORSIKA 7.6400 [8]. Furthermore, we generated cosmic-ray air showers assuming the same source orbit and considered their isotropic characteristics by correcting the number of events using the weighting method described in [5]. As a chemical composition model of cosmic rays, we used the Shibata model [9]. We generated  $10^9$  cosmic-ray events ranging from 300 GeV to 10 PeV. Regarding the hadronic interaction models in air shower generation, we employed QGSJET-II-04 [10], EPOS\_LHC v3400 [11], SIBYLL 2.3c01 [12, 13] at high energies ( $>80$  GeV), and FLUKA [14] and UrQMD [15] at low energies ( $<80$  GeV). First, to investigate whether the low-energy models might cause any significant differences, we performed a Monte Carlo simulation using QGSJET-II-04 combined with FLUKA and QGSJET-II-04 combined with UrQMD. Then, we compared the following four combinations of interaction models: QGSJET-II-04 combined with FLUKA 2011.2x (QGSJET-II + FLUKA), QGSJET-II-04 combined with UrQMD 1.3\_cors (QGSJET-II + UrQMD), EPOS LHC v3400 combined with FLUKA 2011.2x (EPOS\_LHC + FLUKA), and SIBYLL 2.3c01 combined with FLUKA 2011.2x (SIBYLL + FLUKA). Each incident particle is randomly injected within a 300 m radius from the center of the air shower array.

## 2.2 Detector simulation of ALPAQUITA

Using a Monte Carlo simulation of ALPAQUITA [5] implemented in GEANT 4.10.02, we investigated the effect of the four hadronic interaction models described in Section 2.1 on gamma-ray efficiency. ALPAQUITA is a prototype detector for a new experiment ALPACA [6] [7] and in operation from 2022 on the Chacaltaya plateau (4,740 m a.s.l.,  $16^\circ.23'S$ ,  $68^\circ.08'W$ ) in Bolivia. At 15 m intervals, 97 plastic scintillation detectors with an area of  $1 \text{ m}^2$  are arranged, which effective array area is  $18,450 \text{ m}^2$ .

The air shower array measures electrons, gamma rays, and charged particles, their total energy loss is converted to the particle number density  $\rho$  ( $\text{m}^{-2}$ ). The primary energy is calculated from the sum of particle number densities from all detectors,  $\sum \rho$ . Based on the relative hit timing of each detector, we reconstruct the arrival direction of the primary particle using an air shower front surface, approximated with a cone [2]. The selection conditions described in [5] are imposed to analyze the air shower array data.

An underground water Cherenkov-type muon detector (MD) is installed 2 m below the surface air shower array. The MD comprises 16 water tanks (total area of  $900 \text{ m}^2$ ), and each tank has an air layer of 0.9 m, a water depth of 1.5 m, an area of about  $56 \text{ m}^2$ . The concrete ceiling thickness is 20 cm, the thickness of concrete walls is 30 cm. The details of ALPAQUITA are described in [5].

## 2.3 Systematic difference in gamma survival ratio ( $R_i^{\text{surv}}$ ) due to the hadronic interaction model

### 2.3.1 Separation method

The MD detects Cherenkov photons reflected by the tank walls and floor by one PMT mounted downward on the ceiling [5]. The number of photoelectrons peaks at  $\sim 24$  when a single muon

passes through the water tank. We defined this value as one particle, calculate the number of muons  $\sum N_\mu$ , and use it to select a gamma-ray-induced air shower.

Fig. 1a shows a  $\sum \rho$  vs.  $\sum N_\mu$  scatter plot using the QGSJET-II + FLUKA model. As shown in this figure, cosmic rays distribute in the upper region and the gamma rays distribute in the lower region. Figs. 1b, c, and d show the same trend as the QGSJET-II + FLUKA model, with the QGSJET-II + UrQMD model, EPOS\_LHC + FLUKA model, and SIBYLL + FLUKA model, respectively. Fig. 2 shows the number of muon distributions for  $100 < \sum \rho < 178$ , corresponding to a representative energy of  $\sim 56$  TeV.

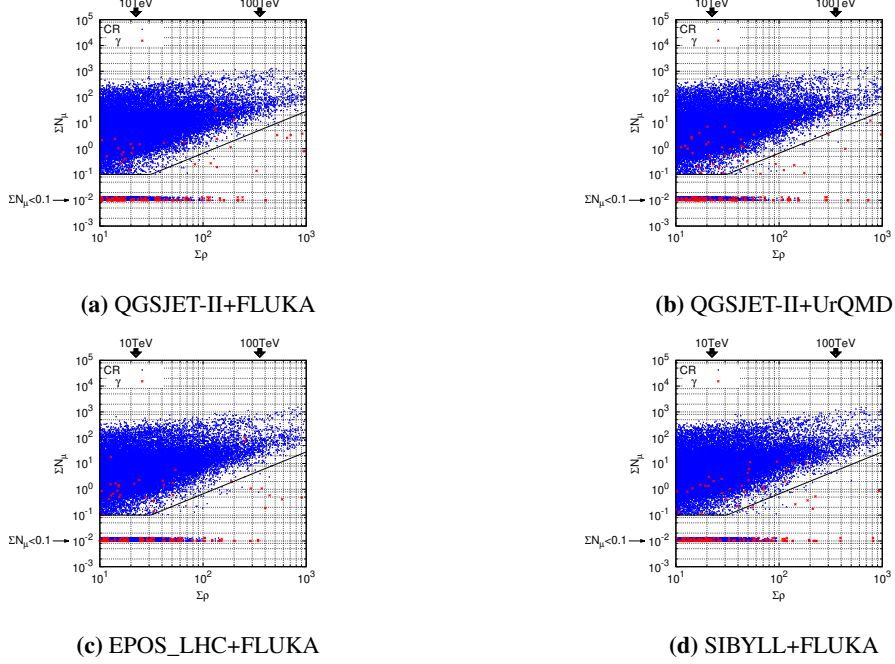


**Figure 1:** Expected  $\sum \rho$  vs.  $\sum N_\mu$  scatter plots of gamma-ray (red) and cosmic-ray (blue) events. Events with  $\sum N_\mu < 0.1$  are artificially piled up around  $\sum N_\mu = 0.01$  distributed randomly within a width of  $0.01 \sim 0.014$ . Each of the four figures shows the results calculated with the different hadronic interaction models. The arrows over the upper horizontal axis show the corresponding gamma-ray energies, 10 TeV and 100 TeV. The solid black line indicates the optimal cut line determined by the method to separate between gamma-ray and cosmic-ray events, described in [5].

As shown in Fig. 2, the  $\sum N_\mu$  of a gamma-ray-induced air shower is obviously smaller than that of a cosmic-ray-induced air shower with the same  $\sum \rho$ .

Events with  $\sum N_\mu < 0.1$  are artificially piled up at  $\sum N_\mu = 0.01$ , where majority of gamma rays are contained. We define gamma-like events below the threshold and cosmic-ray-like events above the threshold using a threshold value of  $\sum N_\mu$  ( $\sum N_{\mu, cut}$ ). We fitted the relationship to the following equation:

$$f(x) = \begin{cases} 0.1 & (x < \sum \rho_0) \\ 0.1 \times \left(\frac{x}{\sum \rho_0}\right)^b & (x \geq \sum \rho_0) \end{cases} \quad (2)$$

In the case of QGSJET-II + FLUKA, the optimal cut line is the solid black line shown in Fig. 1, where  $b$  becomes 1.6 with a fixed  $\sum \rho_0 = 31.2$  [5]. Utilizing the optimal cut line shown in Fig. 2,

we obtained a survival ratio of  $\sim 0.75$  for all models at the representative energy of  $\sim 56$  TeV.

[Model dependence of gamma survival ratio ( $R_i^{\text{surv}}$ )]

As shown in Fig. 1, we calculated  $R_i^{\text{surv}}$  using the optimal cut line obtained with the QGSJET-II + FLUKA model to investigate the differences in  $R_i^{\text{surv}}$ 's due to the hadronic interaction models. After selecting gamma-ray events using the optimal cut line, we obtained  $R_i^{\text{surv}}$ , as shown in Fig. 3.

As shown in Fig. 3,  $R_i^{\text{surv}}$  varies from 0.7 to 0.9 as a function of  $\sum \rho$ , and is  $7.3 \times 10^{-1}$  at 10.9 TeV and  $8.8 \times 10^{-1}$  at 135.9 TeV. To evaluate the differences in  $R_i^{\text{surv}}$  caused by hadronic interaction models, we defined the relative change  $\mathcal{R}(R_i^{\text{surv}})$  to the QGSJET-II + FLUKA model using the following equation:

$$\mathcal{R}(R_i^{\text{surv}}) = \frac{R_i^{\text{surv}} - R_{i=1}^{\text{surv}}}{R_{i=1}^{\text{surv}}} \quad (3)$$

where  $i = 1, 2, 3$ , and 4 represent QGSJET-II + FLUKA, QGSJET-II + UrQMD, EPOS\_LHC + FLUKA and SIBYLL + FLUKA, respectively. The  $\mathcal{R}$  for each model in the energy range between 6 TeV and 300 TeV varies by less than  $\pm 3 \times 10^{-2}$ . As shown in Fig. 3,  $\mathcal{R}$  deviates from zero by  $5.5 \times 10^{-3} \pm 1.2 \times 10^{-2}$ , for the SIBYLL + FLUKA model ( $i = 4$ ), assuming the optimal cut line, and by  $2.0 \times 10^{-3} \pm 9.5 \times 10^{-3}$  for the QGSJET-II + UrQMD model ( $i = 2$ ). The  $\chi^2$  values of the three fitted lines are 6.3, 7.8, and 9.0 (DOF=7), and the upper cumulative probabilities correspond to 0.50, 0.35, and 0.25, respectively, indicating no significant energy dependence.

We estimated the final hadronic interaction model dependence. The final hadronic interaction model dependence includes conservatively differences among the models in the high-energy region [the average fitting result  $\overline{\mathcal{R}(R_{i=4}^{\text{surv}})} = 5.5 \times 10^{-3} \pm 1.2 \times 10^{-2}_{\text{MCstat}}$  and bin-by-bin maximum difference  $(\mathcal{R}(R_{i=4}^{\text{surv}}))_{\text{max}} = 2.2 \times 10^{-2} \pm 1.1 \times 10^{-2}_{\text{MCstat}}$ ] and differences among the models in the low-energy region [the average fitting result  $\overline{\mathcal{R}(R_{i=2}^{\text{surv}})} = 2.0 \times 10^{-3} \pm 9.5 \times 10^{-3}_{\text{MCstat}}$  and bin-by-bin maximum difference  $(\mathcal{R}(R_{i=2}^{\text{surv}}))_{\text{max}} = 1.8 \times 10^{-2} \pm 1.0 \times 10^{-2}_{\text{MCstat}}$ ]. We then estimate the final hadronic interaction model dependence, adding the differences above in quadrature,

$$\begin{aligned} & \sqrt{\overline{(\mathcal{R}(R_{i=4}^{\text{surv}}) + \mathcal{R}(R_{i=2}^{\text{surv}}))^2} + \overline{\mathcal{R}(R_{i=4}^{\text{surv}})}_{\text{MCstat}}^2 + (\mathcal{R}(R_{i=4}^{\text{surv}}))_{\text{max}}^2 + (\mathcal{R}(R_{i=4}^{\text{surv}}))_{\text{max,MCstat}}^2} \\ & \quad \sqrt{\overline{\mathcal{R}(R_{i=2}^{\text{surv}})}_{\text{MCstat}}^2 + (\mathcal{R}(R_{i=2}^{\text{surv}}))_{\text{max}}^2 + (\mathcal{R}(R_{i=2}^{\text{surv}}))_{\text{max,MCstat}}^2} \\ & = 3.6 \times 10^{-2} \end{aligned}$$

We obtained the final hadronic interaction model dependence of less than  $3.6 \times 10^{-2}$ , which is dominated by Monte Carlo statistics.

### 3. Conclusion

Using an extensive air shower array and an underground muon detector to measure high-energy gamma ray, we studied the performance of a hybrid experiment. The experiment separates between gamma-ray-induced muon-poor air showers and cosmic-ray-induced muon-rich air showers using an underground muon detector. To investigate the performance of this type of experiment, such as

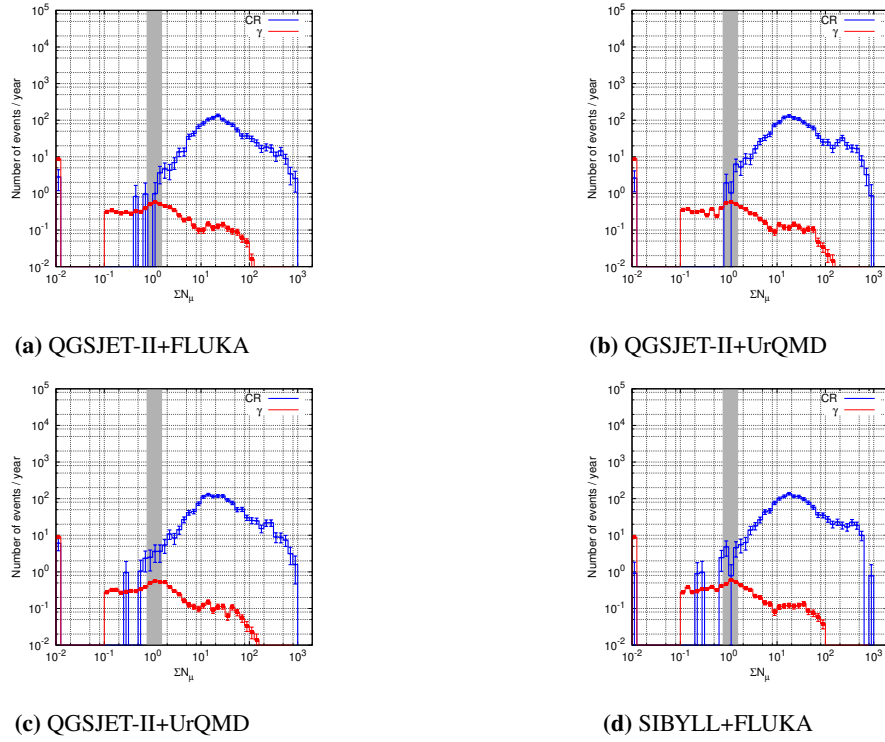


**Figure 2:** Expected numbers of gamma-ray and cosmic-ray induced air showers per year by ALPAQUITA as a functions of the number of detected muons  $\sum N_\mu$  for  $100 < \sum \rho < 178$  corresponding to the gamma-ray equivalent energy  $E_\gamma$  of 56 TeV. The red histograms indicate gamma-ray induced air shower events, and the blue histograms show cosmic-ray induced air shower events. Each of the four figures show the results calculated with a different hadronic interaction model, (a) QGSJET-II + FLUKA, (b) QGSJET-II + UrQMD, (c) EPOS\_LHC + FLUKA, and (d) SIBYLL + FLUKA, respectively. Events with  $\sum N_\mu < 0.1$  are artificially piled up at  $\sum N_\mu = 0.01$ . The shaded gray band indicates the threshold values of  $\sum N_\mu$  which depend on  $\sum \rho$ , as shown in Fig 1.

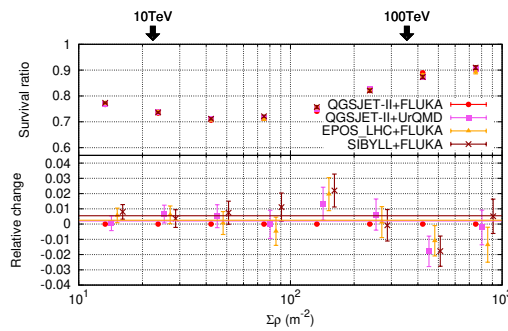


**Figure 3:** Expected survival ratio of gamma-ray events after applying the  $\sum N_\mu$  selection criterion (see the black lines shown in Fig. 1) and  $\mathcal{R}$  (the survival ratio relative to the QGSJET-II + FLUKA model) as a function of  $\sum \rho$ , assuming the optimal survival line in Fig. 1 in ALPAQUITA. Each horizontal straight line results from fitting the  $\mathcal{R}$  to a constant value for each model (QGSJET-II + UrQMD, EPOS\_LHC + FLUKA, and SIBYLL + FLUKA). The arrows over the upper horizontal axis show the corresponding gamma-ray energies, 10 TeV and 100 TeV. Adapted from [16]

ALPAQUITA, a Monte Carlo simulation of air showers based on hadronic interaction models is required. This simulation might have some model dependence. Air shower experiments such as ALPAQUITA estimate the gamma-ray flux from the difference between the number of on-source and off-source event by real data, using the gamma-ray detection efficiency calculated by a Monte Carlo simulation, which depends on the hadronic interaction models, whereas the off-source, background cosmic-ray events, can be estimated experimentally. In particular, the models affect the number of muons in the gamma-ray-induced air showers.

Thus, we evaluate the hadronic interaction model dependence in the gamma-ray flux measurements between 6 and 300 TeV with the four models—QGSJET-II + FLUKA, QGSJET-II + UrQMD, EPOS\_LHC + FLUKA, and SIBYLL + FLUKA.

Using the ALPAQUITA simulated detector, we evaluated the impact of these small differences in the characteristics of air shower muons on the gamma-ray flux estimation. For optimal cut line obtained with QGSJET-II + FLUKA, the survival ratio of gamma-ray events varied from 0.7 to 0.9 for  $\sum \rho$  in the energy range from 6 to 300 TeV. Thus, the survival ratio's model dependence is less than 3.6 % in the energy range from 6 to 300 TeV. The survival ratio is used in the flux calculation in the form of  $(R_i^{\text{surv}})^{-1}$ ; thus, the model dependence in the flux estimation is of the same magnitude, which is dominated by Monte Carlo statistics. The contribution of the hadronic interaction model dependence to the gamma-ray flux estimation is negligible compared to other systematic errors, such as the energy scale uncertainty (typically  $\sim 10\%$ ) corresponding to the 20 %-30 % gamma-ray flux uncertainty. Furthermore, as Monte Carlo statistics account for most of the 3.6 % uncertainty due to hadronic interaction model dependence, it is projected to be significantly less than 3.6 %.

## Acknowledgements

The ALPACA project is supported by the Japan Society for the Promotion of Science (JSPS) through Grants-in-Aid for Scientific Research (A) 19H00678, Scientific Research (B) 19H01922, Scientific Research (B) 20H01920, Scientific Research (S) 20H05640, Scientific Research (B) 20H01234, Scientific Research (B) 22H01234, Scientific Research (C) 22K03660 and Specially Promoted Research 22H04912, the LeoAtrox supercomputer located at the facilities of the Centro de Análisis de Datos (CADS), CGSAIT, Universidad de Guadalajara, México, and by the joint research program of the Institute for Cosmic Ray Research (ICRR), The University of Tokyo. Y. Katayose is also supported by JSPS Open Partnership joint Research projects F2018, F2019. K. Kawata is supported by the Toray Science Foundation. E. de la Fuente thanks financial support from Inter-University Research Program of the Institute for Cosmic Ray Research, The University of Tokyo, grant 2023i-F-005. I. Toledano-Juarez acknowledges support from CONACyT, México; grant 754851.

## References

- [1] Sinnis G.: Air shower detectors in gamma-ray astronomy. *New J. Phys.*, **11**, 055007 (2009)
- [2] Amenomori, M. et al.: First Detection of Photons with Energy beyond 100 TeV from an Astrophysical Source. *Phys. Rev. Lett.*, **123**, 05113 (2019)

- [3] Sako T.K. et al.: Exploration of a 100 TeV gamma-ray northern sky using the Tibet air-shower array combined with an underground water-Cherenkov muon-detector array. *Astroparticle Phys.*, **32**, 177 (2009)
- [4] Amenomori, M. et al.: Search for Gamma rays above 100 TeV from the Crab Nebula with the Tibet Air shower Array and the 100 m<sup>2</sup> Muon Detector. *ApJ*, **813**, 98 (2015)
- [5] S. Kato et al.: Detectability of southern gamma-ray sources beyond 100 TeV with ALPAQUITA, the prototype experiment of ALPACA. *Exp. Astron.*, **52**, 85 (2021)
- [6] Calle C. et al.: Expected performance of the prototype experiment for the ALPACA experiment. *PoS(ICRC2019)* 711 (2019)
- [7] Calle C. et al.: ALPACA air shower array to explore 100 TeV gamma-ray sky in Bolivia. *PoS(ICRC2019)* 779 (2019)
- [8] Heck D. et al.: CORSIKA: A Monte Carlo code to simulate extensive air showers. Forschungszentrum Karlsruhe Report FZKA 6019 (1998)
- [9] M. Shibata et al.: Chemical Composition and Maximum Energy of Galactic Cosmic Rays. *ApJ*, **716**, 1076 (2010)
- [10] Ostapchenko S.: QGSJET-II: towards reliable description of very high energy hadronic interactions. *Nucl. Phys. B (Proc. Suppl.)*, **151**, 143 (2006)
- [11] Pierog T. et al.: EPOS LHC: Test of collective hadronization with data measured at the CERN Large Hadron Collider. *Phys. Rev. C* , **92**, 034906 (2015)
- [12] R. Enge .et al.: The hadronic interaction model Sibyll ? past, present and future. *EPJ Web of Conferences* , **145**, 08001 (2017)
- [13] A. Fedynitch .et al.: Hadronic interaction model sibyll 2.3c and inclusive lepton fluxes. *Phys. Rev. D*, **100**, 103018 (2019)
- [14] Battistoni G.et al.: Overview of the FLUKA code. *Annals of Nuclear Energy*, **82**, 10 (2015)
- [15] Bleicherda M. et al.: Relativistic hadron-hadron collisions in the ultra-relativistic quantum molecular dynamics model. *J. Phys. G: Nucl. Part.*, **25**, 1859 (1999)
- [16] S.Okukawa et al.: Hadronic interaction model dependence in cosmic Gamma-ray flux estimation using an extensive air shower array with a muon detector. *Exp. Astron.*, **55**, 325 (2022)



**Full Authors List: ALPACA Collaboration**

M. Anzorena<sup>1</sup>, D. Blanco<sup>2</sup>, E. de la Fuente<sup>3,4</sup>, K. Goto<sup>5</sup>, Y. Hayashi<sup>6</sup>, K. Hibino<sup>7</sup>, N. Hotta<sup>8</sup>, A. Jimenez-Meza<sup>9</sup>, Y. Katayose<sup>10</sup>, C. Kato<sup>6</sup>, S. Kato<sup>1</sup>, I. Kawahara<sup>10</sup>, T. Kawashima<sup>1</sup>, K. Kawata<sup>1</sup>, T. Koi<sup>11</sup>, H. Kojima<sup>12</sup>, T. Makishima<sup>10</sup>, Y. Masuda<sup>6</sup>, S. Matsuhashi<sup>10</sup>, M. Matsumoto<sup>6</sup>, R. Mayta<sup>13,14</sup>, P. Miranda<sup>2</sup>, A. Mizuno<sup>1</sup>, K. Munakata<sup>6</sup>, Y. Nakamura<sup>1</sup>, C. Nina<sup>2</sup>, M. Nishizawa<sup>15</sup>, R. Noguchi<sup>10</sup>, S. Ogio<sup>1</sup>, M. Ohnishi<sup>1</sup>, S. Okukawa<sup>10</sup>, A. Oshima<sup>5,11</sup>, M. Raljevich<sup>2</sup>, T. Saito<sup>16</sup>, T. Sako<sup>1</sup>, T. K. Sako<sup>1</sup>, J. Salinas<sup>2</sup>, T. Sasaki<sup>7</sup>, T. Shibusaki<sup>17</sup>, S. Shibata<sup>12</sup>, A. Shiomi<sup>17</sup>, M. A. Subieta Vasquez<sup>2</sup>, N. Tajima<sup>18</sup>, W. Takano<sup>7</sup>, M. Takita<sup>1</sup>, Y. Tameda<sup>19</sup>, K. Tanaka<sup>20</sup>, R. Ticona<sup>2</sup>, I. Toledano-Juarez<sup>21,22</sup>, H. Tsuchiya<sup>23</sup>, Y. Tsunesada<sup>13,14</sup>, S. Udo<sup>7</sup>, R. Usui<sup>10</sup>, R. I. Winkelmann<sup>2</sup>, K. Yamazaki<sup>11</sup> and Y. Yokoe<sup>1</sup>

<sup>1</sup>Institute for Cosmic Ray Research, University of Tokyo, Kashiwa 277-8582, Japan.

<sup>2</sup>Instituto de Investigaciones Físicas, Universidad Mayor de San Andrés, La Paz 8635, Bolivia.

<sup>3</sup>Departamento de Física, CUCEI, Universidad de Guadalajara, Guadalajara, México.

<sup>4</sup>Doctorado en Tecnologías de la Información, CUCEA, Universidad de Guadalajara, Zapopan, México.

<sup>5</sup>College of Engineering, Chubu University, Kasugai 487-8501, Japan.

<sup>6</sup>Department of Physics, Shinshu University, Matsumoto 390-8621, Japan.

<sup>7</sup>Faculty of Engineering, Kanagawa University, Yokohama 221-8686, Japan.

<sup>8</sup>Faculty of Education, Utsunomiya University, Utsunomiya 321-8505, Japan.

<sup>9</sup>Departamento de Tecnologías de la Información, CUCEA, Universidad de Guadalajara, Zapopan, México.

<sup>10</sup>Faculty of Engineering, Yokohama National University, Yokohama 240-8501, Japan.

<sup>11</sup>College of Science and Engineering, Chubu University, Kasugai 487-8501, Japan.

<sup>12</sup>Chubu Innovative Astronomical Observatory, Chubu University, Kasugai 487-8501, Japan.

<sup>13</sup>Graduate School of Science, Osaka Metropolitan University, Osaka 558-8585, Japan.

<sup>14</sup>Nambu Yoichiro Institute for Theoretical and Experimental Physics, Osaka Metropolitan University, Osaka 558-8585, Japan.

<sup>15</sup>National Institute of Informatics, Tokyo 101-8430, Japan.

<sup>16</sup>Tokyo Metropolitan College of Industrial Technology, Tokyo 116-8523, Japan.

<sup>17</sup>College of Industrial Technology, Nihon University, Narashino 275-8575, Japan.

<sup>18</sup>RIKEN, Wako 351-0198, Japan.

<sup>19</sup>Faculty of Engineering, Osaka Electro-Communication University, Neyagawa 572-8530, Japan.

<sup>20</sup>Graduate School of Information Sciences, Hiroshima City University, Hiroshima 731-3194, Japan.

<sup>21</sup>Doctorado en Ciencias Físicas, CUCEI, Universidad de Guadalajara, Guadalajara, México.

<sup>22</sup>Maestría en Ciencia de Datos, Departamento de Métodos Cuantitativos, CUCEA, Universidad de Guadalajara, Zapopan, México.

<sup>23</sup>Japan Atomic Energy Agency, Tokai-mura 319-1195, Japan.